Invited Paper

Coherence in UV resonance Raman spectroscopy of liquid benzene and toluene, but not ice

Hans D. Hallen*[a], Ryan R. Neely III[a], Adam H. Willitsford[b], C. Todd Chadwick[a], C. Russell Philbrick[a]

[a]North Carolina State University, Department of Physics, Raleigh, NC, USA 27695-8202;
[b]Johns Hopkins University Applied Physics Laboratory, Laurel, MD USA 20709

ABSTRACT

We have measured UV resonance Raman scattering at and near the resonance absorption lines of liquid benzene and toluene. Resonance occurs for excitation on the symmetry-forbidden but strongly phonon coupled states in the $^1B_{2u}$ band, ~230-270 nm, resulting in enhancements corresponding to the vapor phase absorptions rather than those of the liquid phase. This effect is related to the coherence forced by the internal molecular resonance required to absorb light at this energy. The resonance gains (~1000x) are larger than expected due to the narrower vapor phase lines. Several multiplet and overtone modes are enhanced along with the strongly coupled ring-breathing mode. A contrasting case of resonance Raman of ice is also discussed; in this case resonance is observed for excitation energy corresponding to absorptions that depend upon the final state shielding by the neighbors, and corresponds with the solid phase absorption. This typifies the more common, slow, time dependence of the resonance Raman process.

Keywords: resonance Raman, benzene, toluene, forbidden transition

1. INTRODUCTION

Raman spectroscopy has become a commonly used tool for substance identification [1-3], stress measurements [4], and material characterization. Resonance Raman occurs when the excitation laser is tuned to an absorption feature of the material to be studied. It is useful in increasing signal levels for trace materials in a non-absorbing matrix or for nanoscale studies, which are limited in both volume and number of molecules available [5-11]. Many studies have used fix laser wavelengths to study pre-resonance Raman, in which the Raman signal is enhanced, but the excitation is not precisely at the absorption energy [12-17]. In this study, we tune the excitation laser in fine steps across the absorption features of interest. The enhancement is usually described qualitatively as due to the longer timescale of the resonance Raman process compared to normal Raman since the resonant case involves a real intermediate state rather than a virtual state. For the case of the virtual state, the timescale of the process is limited by the Heisenberg uncertainty principle, and is essentially instantaneous compared to the atomic motion. In this report, we find that the resonance Raman process can be very short when the excitation is tuned to a symmetry forbidden transition, although the resonance gain is still large. We attribute this to the fact that a phonon must be available to allow absorption at that energy, and this requires a resonance within the molecule itself, which is short-lived. We observe it as the resonance gain for a liquid sample associated with the vapor-phase absorption rather than the liquid phase absorption. When the process is short compared to the time a molecule interacts with its neighbors, the molecule will appear to have vapor phase energy transitions. Note that the molecule itself sets the time scale, not the laser pulse length or the time to exchange energy with its neighbors. Also note that the molecule is not in the vapor phase, and will not appear so when probed with a longer-timed process, such as absorption. The dielectric constant, defined in frequency, assumes a longer-timed process and cannot be used to describe this short-timed interaction. To contrast this case, we also present data of resonance Raman of ice. We find resonance gain occurring in a broad wavelength excitation band, 220-270 nm. Absorption at these wavelengths is observed in ice, but not water vapor, which absorbs strongly at shorter wavelengths. The reduction of the absorption energy in ice is due to a shielding of the absorption-induced dipole by movement of the dipoles of its neighbors. In other words, absorption at that energy relies upon interaction with the neighboring molecules. We observe resonance at this feature of ice since it is an allowed absorption energy in ice; thus, the typical resonance Raman process is long compared to the interaction time with its neighbors.

Ultrafast Imaging and Spectroscopy, edited by Zhiwen Liu, Proc. of SPIE Vol. 8845, 884511 · © 2013 SPIE · CCC code: 0277-786X/13/$18 · doi: 10.1117/12.2024313

*Hans_Hallen@ncsu.edu; phone 1 919-515-6314

2. METHODS

Raman measurements of both liquids and solids are made in a 90-degree geometry with laser incident from underneath the sample, so that there is no presence of vapor in the beam path for the liquid measurements [9-10]. The tunable deep-UV laser is based upon frequency doubling of the output of an optical parametric oscillator (OPO) (Uoplaz) pumped by the third harmonic of a ND-YAG laser (Spectra Physics). As shown in Fig. 1(a), the Nd-YAG laser output is tripled and a Pellin-Broca prism used to choose only the third harmonic beam to enter the OPO section, Fig. 1(b). The OPO uses a counter-rotating quartz rod outside the cavity to correct lateral motion of the beam induced by the rotation of the BBO nonlinear crystal during wavelength adjustment. One of two BBO crystals, also counter-rotating, is used to double the OPO output frequency. A Pellin-Broca prism is used to choose the wavelength and aim the beam. The usable DUV range of wavelengths is ~215 – 300 nm, with visible wavelengths from the non-doubled outputs and near infrared from the idler output.

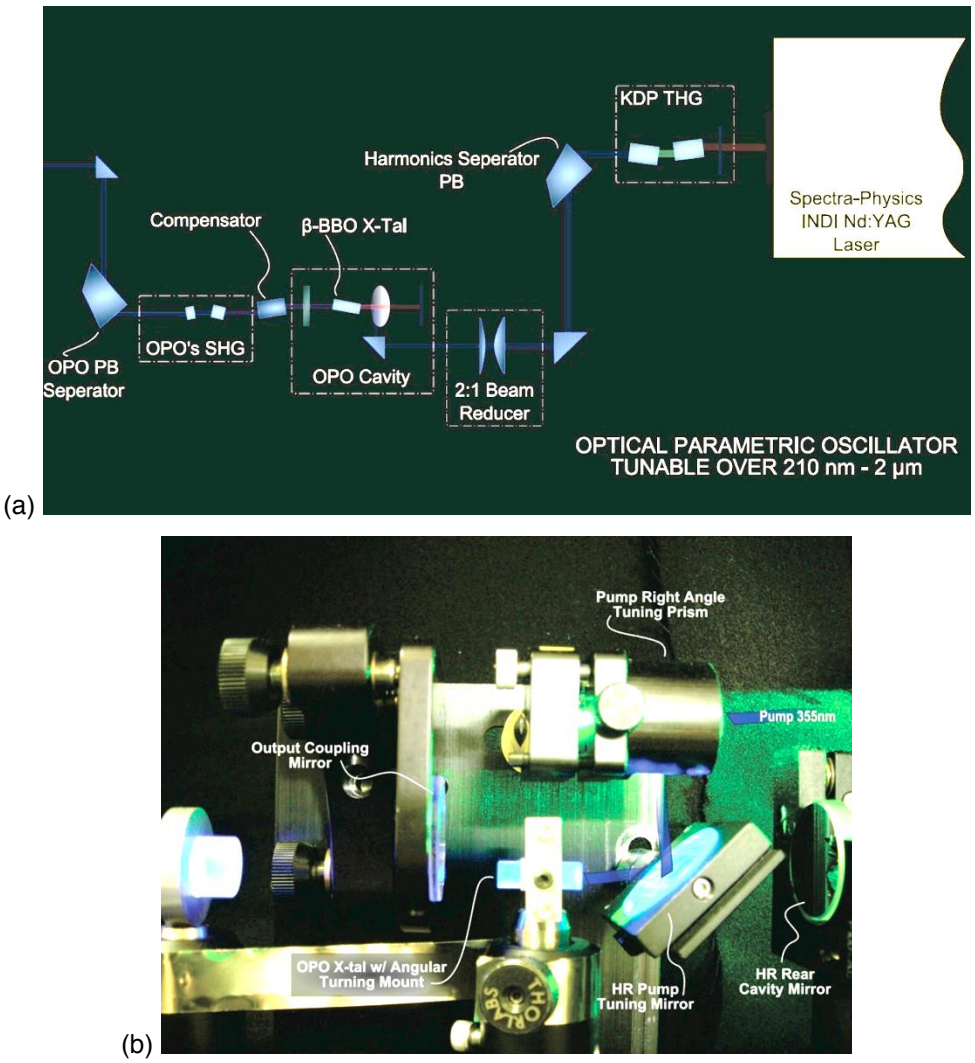

Figure 1. (a) Tunable laser system is shown schematically (b) Photograph of the critical OPO stage.[8-10].

The sample configuration of the 90-degree optical scattering geometry used for collection of the Raman spectra is shown in Fig. 2. Liquid samples are observed through a fused silica window at the bottom of a Teflon sample holder. A Peltier cooling unit that constantly condenses and freezes atmospheric water vapor produces the ice sample. Light is collected and coupled into a Spex Triplemate 1877 three-stage spectrometer. The first two stages form a small subtractive unit to filter fluorescent background and other stray light, while a longer third stage disperses the Raman signal across an Andor EM-CCD camera.

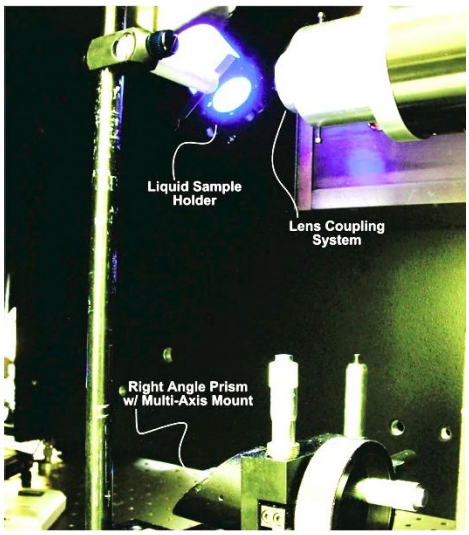

Figure 2. The signal collection from the sample is in a 90 degree configuration. Laser light enters from the left at the bottom and approaches the sample from the bottom. The collection optics are visible in the upper right. The sample in this picture is for the liquids, using bottom-side illumination to preclude vapor measurements.

3. RESULTS

Several Raman spectra obtained for a very narrow range of excitation wavelengths are shown in Fig. 3. Since we are interested in enhancement of the Raman signals due to the resonance effect, we normalize all spectra for laser power and the non-resonant ν_0^4 dipole emission enhancement. The Raman signal is very small for the shortest excitation wavelength used. As the excitation wavelength increases, the intensity of the Raman lines is observed to increase, then decrease, then increase again. This strong dependence on excitation energy is not expected for a condensed liquid system, for which line widths are normally much broader. In fact, if the resonance signal levels are compared to liquid and gas phase absorption, one finds almost no correlation to the nearly flat liquid absorption in this range (it increases with wavelength to a maximum several nanometers longer that the region studied here), and exhibits a strong correlation to the vapor phase absorption.

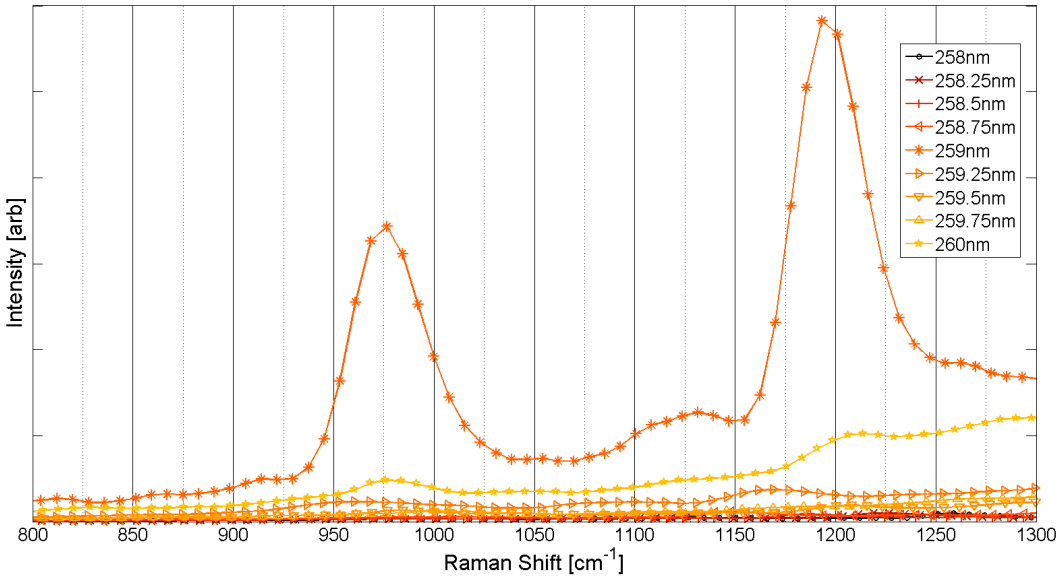

Figure 3. Raman spectra of liquid benzene over a 2 nm range of excitation wavelength in which the liquid absorption is featureless, but the vapor phase absorption has peaks [8].

The Raman spectra of toluene also vary in intensity as the excitation energy is tuned over a narrow range of wavelengths, and follows the vapor phase absorption, Fig. 4. The liquid toluene measurement shows the same type of resonance associated with the forbidden transitions observed in benzene and other cyclic hydrocarbons, where the resonance excitations occur at the vapor absorption features. Raman spectra from ice with excitation wavelengths from 215 nm to 430 nm are shown in Fig. 5. The ice contrasts with a broad wavelength range of lower level excitation that corresponds to the liquid absorption.

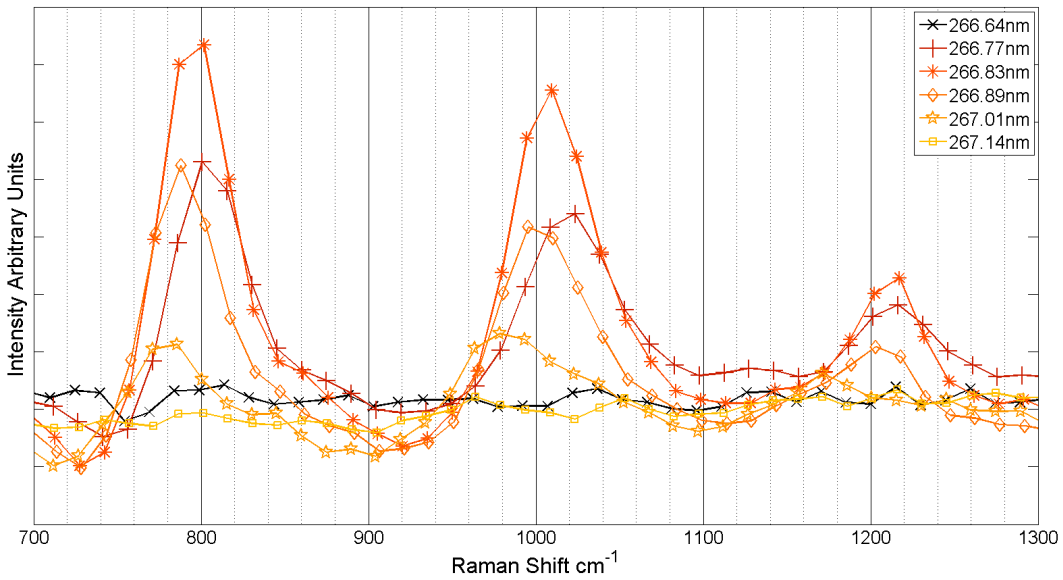

Figure 4. Raman spectra of liquid toluene over a 0.5 nm range of excitation wavelength in which the liquid absorption is featureless, but the vapor phase absorption has peaks.

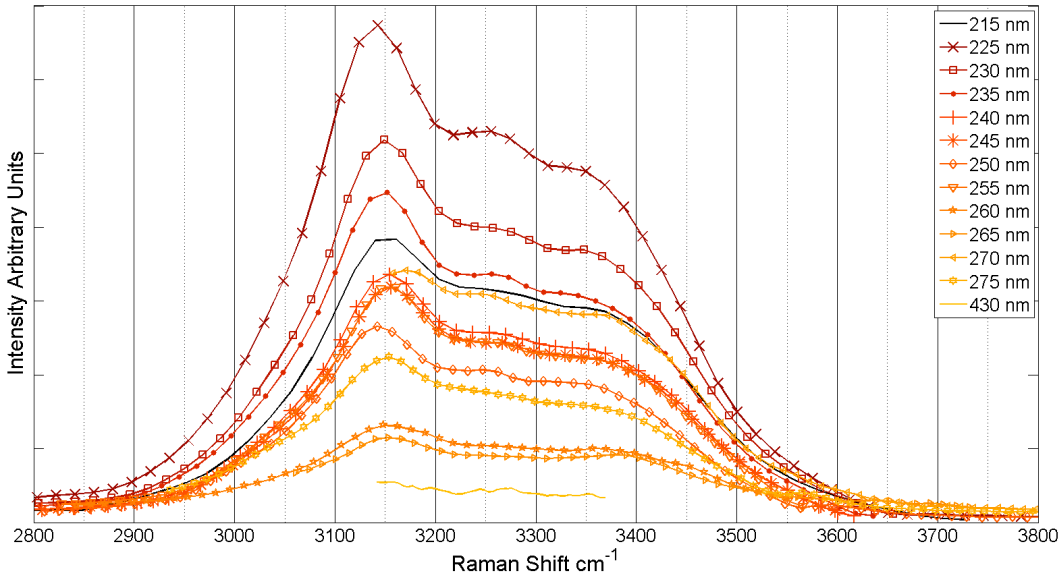

Figure 5. The Raman spectra of ice in small steps of excitation energy from 215 – 277.5 nm, and also the Raman spectra with excitation of 430 nm as a reference.

The Raman signals shown in Fig. 5 have the three-peak structure expected for ice [18-20]. The Raman signal in the visible (439 nm) is small, and is only slightly larger at 277 nm. It increases rapidly near 263 nm, then more slowly again until it decreases near 250 nm, and then continues to rise again. The increase in the Raman signals is not monotonic, as is evident in the figure. To illustrate these points, the areas under the Raman spectra in Fig. 5 are integrated, and the sums are plotted in Fig. 6. The x-axis is in wavenumbers rather than in wavelength so that the energy levels are more evident.

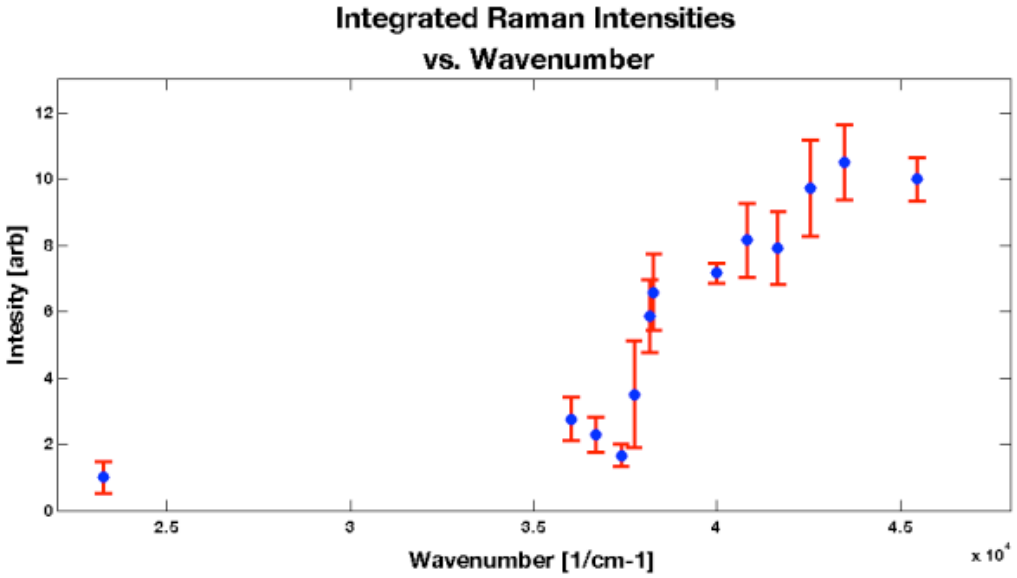

Figure 6. The integrals of Raman spectra of ice in small steps of excitation energy from 215 – 277.5 nm, and also the integral of the Raman spectra with excitation of 430 nm as a reference.

4. ANALYSIS AND DISCUSSION

The structure on the integrated Raman intensity curve in Fig. 6 can be understood as a combination of a pre-resonant contribution of the strong ice absorption at 150 nm with a weaker resonance occurring in the wavelength range studied here. We fit the pre-resonance contribution and subtract it so that the resonance contribution can be observed directly. Usually, Raman scattering has intensity proportional to v_0^4 like dipole absorption/emission. A deviation from this proportionality occurs due to the 'A term' of the Raman scattering tensor α [10], so that as the frequency of the incident light approaches an electronic transition, the intensity I_{fi} for an initial, i, to final, f, state is given by

$$I_{fi} = \left(\frac{\pi}{\epsilon_0}\right)^2 (\nu_0 \pm \nu_{fi})^4 J_0 \sum_{\rho,\sigma} [\alpha_{\rho\sigma}]_{fi} [\alpha_{\rho\sigma}]^{\dagger}_{fi}\,, \tag{1}$$

where the sum is over all possible intermediate states, the resonant frequency is v_{fi}, and the input flux J_0. We take the derivative of the polarizability tensor with respect to the normal coordinate Q_a to obtain

$$\partial(\alpha_{\rho\rho})_{kk}/\partial Q_a = A + B, \tag{2}$$

$$\text{where } A = \frac{1}{h}\sum_r \left(\frac{2\nu_{rk}}{(\nu_{rk}^2 - \nu_0^2)} \frac{\partial |(M_\rho)_{rk}|^2}{\partial Q_a}\right) \text{ and } B = \frac{-2}{h}\sum_r \left(\frac{\nu_{rk}^2 + \nu_0^2}{(\nu_{rk}^2 - \nu_0^2)^2} |(M_\rho)_{rk}|^2 \frac{\partial \nu_{rk}}{\partial Q_a}\right), \tag{3}$$

are the A and B terms. The A term will dominate and the derivative part is not strongly frequency dependent. Usually only one of the terms in the sum will be important when the excitation frequency, v_0, is close to it.

We use this result to build a simple model for our data, normalized for input power and corrected for v_0^4, as a constant plus the dominant contribution to the A term. Our model takes the form:

$$I \propto C[(2\nu_a)^2/(\nu_a^2 - \nu_0^2)^2] + D, \quad (4)$$

where C and D are proportionality constants and ν_a is the representative excitation frequency between the ground state and electronic state.

Applying our model, Eqn. 4, to the first and last several data points of Fig. 6, we fit C, D and ν_a. The representative excitation frequency, ν_a, is 155 nm. This corresponds closely to the first major peak in the far UV absorption of water at 150 nm. This feature of the data is the primary pre-resonant excitation. The fitted data is shown in Fig. 7, where it becomes evident why only the first several and last several points can be used in the fit. Since we have only used one dominant term from the sum in A, we fit only the background while the other terms from the sum in A remain. Several show resonance in the wavelength range studied.

By subtracting from the data the fitted resonance contribution from the 150 nm absorption, we are able to examine the broad (band) resonance that is super imposed on it, see Fig. 8. Note that there is a gap in the resonance gain near the larger wavenumber end, 4.5-4.8 cm^{-1}, and also a sharp dip at 3.7 cm^{-1}. Figure 8 also contains a plot of the energy dependent absorption measured for ice. A strong correlation between the resonantly enhanced band and the absorption curve of ice is observed. Water vapor shows no similar absorption structure beyond the primary resonant effect that occurs below 200 nm. Thus, the absorption band we observe is a solid-state effect. In fact, the energy lowering of the absorption is due to re-arrangement of the neighboring dipoles to reduce the energy of the excited state via a reduction of the field extent of the induced dipole.

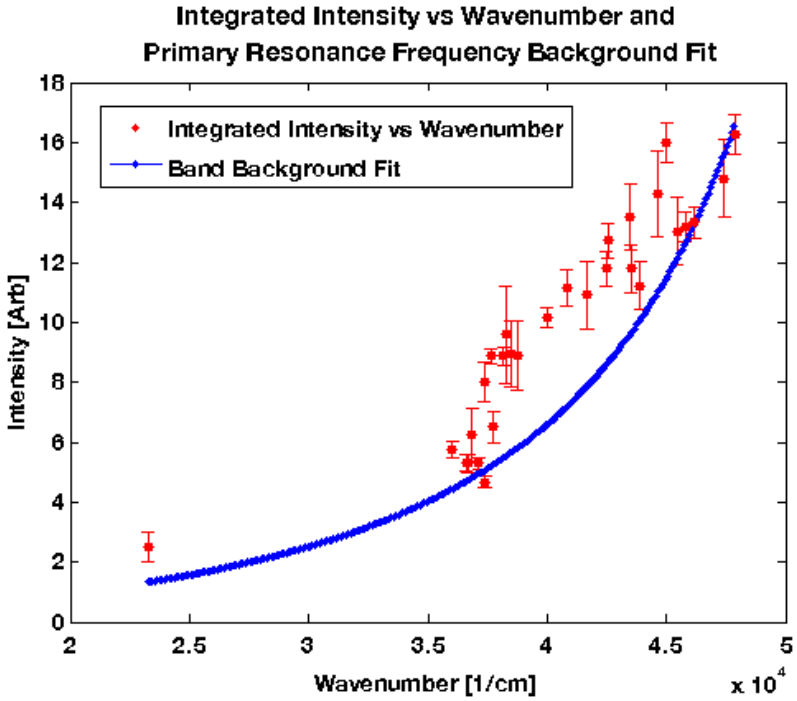

Figure 7. The integrated Raman spectra of ice in small steps of excitation energy from 215 – 277.5 nm, and also the Raman spectra with excitation of 430 nm as a reference.

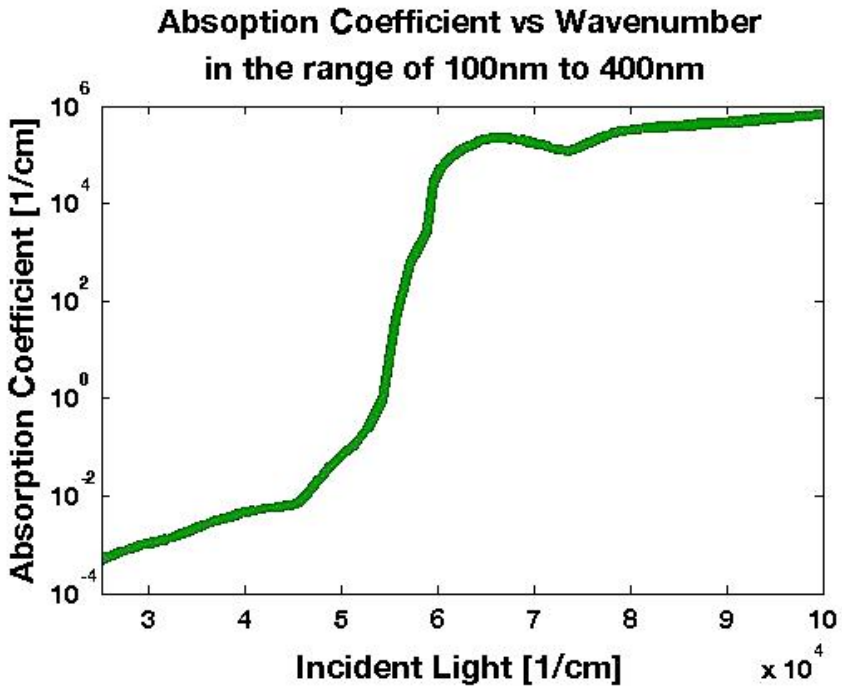

(a)

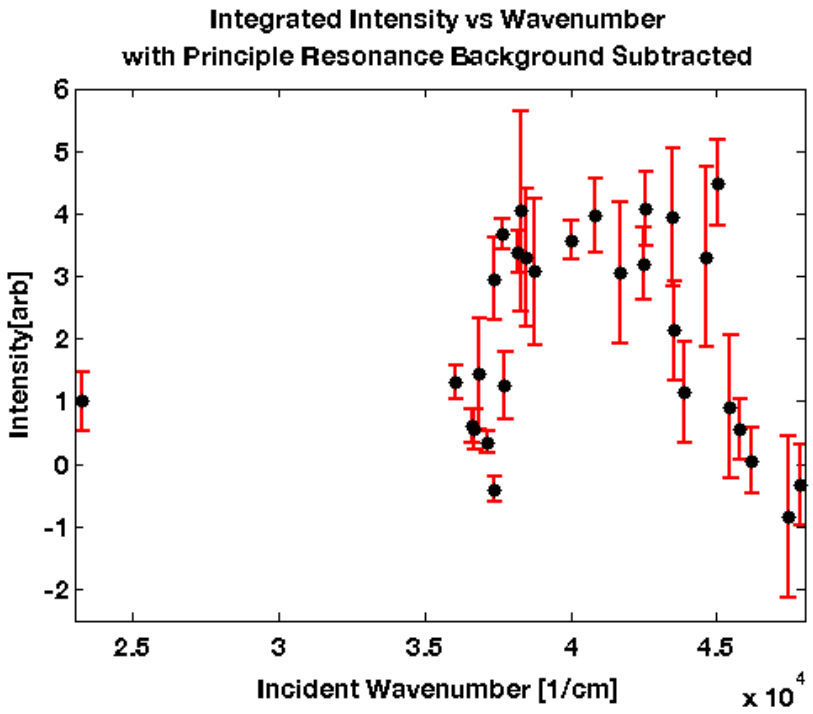

(b)

Figure 8. The resonance from the ice absorption in the wavelength region studied, obtained by subtracting the fitted resonance gain from the 155 nm ice absorption in Fig. 7, is compared to ice absorption curves.

5. CONCLUSIONS

These resonance Raman data demonstrate two different processes. The first, illustrated by benzene and toluene, demonstrates a strong resonance that is due to their forbidden absorption lines, near 259.0 nm in benzene and 266.83 nm in toluene, and it is a very fast process. Therefore, the spectra are coherent in the sense that they depend only upon a single molecule. This is manifested in the fact that the resonance follows the vapor phase absorption lines, which correspond to absorption by non-interacting molecules. The second, illustrated by ice, is a relatively slow process. The interaction with the neighbors is required to obtain absorption at the excitation wavelengths used. We therefore conclude that final state effects are important in the ice system, whereas they are excluded from the benzene and toluene absorption cases. We expect that benzene and toluene also have slow responses when their resonances are probed near allowed states of those molecules.

The implications of these results are far reaching. The narrow resonances afforded by vapor-like resonances generate larger resonance gains than would be achievable with broader condensed phase absorptions. Thus, it opens the possibility of very sensitive measurements of condensed phases. Since the six-member carbon ring is common, the expectation is that all such aromatic compounds will be amenable to usage of these forbidden transitions, which are at relatively convenient wavelengths. Thus, the technique should have broad application.

REFERENCES

1. Sedlacek, A. and Chen, C., "Exploitation of resonance Raman spectroscopy as a remote chemical sensor," *BNL-61359: Conf. 950787-35* (1995).
2. Sedlacek, A. and Chen, C., "Remote detection of trace effluents using resonance Raman spectroscopy. *BNL-49542: Conf. 9311173-2* (1995).
3. Chen, C., Heglund, D., Ray, M., Harder. D., Dobert, R., Leung, K., Wu, M., and Sedlacek, A., "Application of resonance Raman lidar for chemical species identification," *BNL-64388: Conf.-970465-19* (1997).
4. Sparks, R.G., Enloe, W.S., and Paesler, M.A., "Micro-Raman depth analysis of residual stress in machined germanium," Precision Engineering, **13** (3), 189-195 (1991).
5. Chadwick, C. T., Willitsford, A. H., Hallen, H. D., and Philbrick, C. R., "Deep ultraviolet Raman spectroscopy: a resonance-absorption trade-off illustrated by diluted liquid benzene," (manuscript to be published).
6. Hallen, H.D., "Nano-Raman Spectroscopy: Surface Plasmon Emission, Field Gradients, and Fundamentally Near Field Propagation Effects," NanoBiotechnology: **3** (3), 197 (2009).
7. Jahncke, C.L., Paesler, M. A., and Hallen, H.D., "Raman imaging with near-field scanning optical microscopy," Appl. Phys. Lett. **67** (17), 2483-2485 (1995).
8. Willitsford, A., Chadwick, C. T., Hallen, H., and Philbrick, C. R., "Resonance Raman measurements utilizing a tunable deep UV source," *Proc. SPIE Laser Radar Technology and Applications XIII. 6950*-10, 8pp (2008).
9. Willitsford, A., Resonance Raman Spectroscopy in the Ultraviolet using a Tunable Laser, Penn State University Ph.D. Dissertation, (2008) https://etda.libraries.psu.edu/paper/8149/.
10. Chadwick, C. T., Resonance Raman Spectroscopy Utilizing Tunable Deep Ultraviolet Excitation for Materials Characterization, North Carolina State University Ph.D. Dissertation (2009), http://repository.lib.ncsu.edu/ir/bitstream/1840.16/5473/1/etd.pdf .
11. Willitsford, A., Chadwick, C. T., Hallen, H., Kurtz, S., and Philbrick, C. R., "Resonance enhanced Raman scatter in liquid benzene at vapor-phase absorption peaks," (Submitted, in review 2013).
12. Ziegler, L. and Hudson, B., "Resonance Raman scattering of benzene and benzene-d_6 with 212.8 nm excitation," J. Chem. Phys. **74** (2), 982-992 (1981).
13. Asher, S. and Johnson, C., "Resonance Raman excitation profile through the $^1B_{2u}$ state of benzene," J. Phys. Chem. **89**, 1375-1379 (1985).
14. Gerrity, D., Ziegler, L., Kelly, P., Desiderio, R., and Hudson, B., "Ultraviolet resonance Raman spectroscopy of benzene vapor with 220-184 nm excitation," J. Chem. Phys. **83** (7), 3209-3213 (1985).
15. Sension, R., Brudzynski, R., Li, S., and Hudson, B., "Resonance Raman spectroscopy of the B_{1u} region of benzene: analysis in terms of pseudo-Jahn-Teller Distortion," J. Chem. Phys. **96** (4), 2617-2628 (1991).

16. Sension, R., Brudzynski, R., and Hudson, B., "Vacuum ultraviolet resonance Raman studies of the valence electronic states of benzene and benzene-d_6: The E_{1u} state and a putative A_{2u} state," J. Chem. Phys. **94** (2), 873-882 (1990).
17. Ziegler, L. and Albrecht, A., "Raman scattering of benzene in the ultraviolet," J. Chem. Phys. **67** (6), 2753-2757 (1977).
18. Sivakumar, T., Chew, H., and Johari, G., "Effect of pressure on the Raman Spectrum of ice," Nature **27**5, (1978).
19. Mishima, O. and Suzuki, Y., "Propagation of the polyamorphic transition of ice and the liquid-liquid critical point," Nature 419, (2002).
20. Kapitan, J., Hecht, L., and Bour. P., "Raman Spectral evidence of methyl rotation in liquid toluene," Phys. Chem. Chem. Phys. **10**, 1003-1008 (2008).